Seismic Pile Foundation Stiffnesses at Cypress Street Viaduct

G. NORRIS, R. SIDDHARTHAN, Z. ZAFIR, AND P. GOWDA

Given the soil borings, the estimated soil properties, the free-field ground surface motions (at strong-motion stations on either side of the Cypress Street viaduct in Oakland, California), and the assessed buildup in porewater pressure in the Merritt sand discussed in the preceding paper in this Record, the nonlinear variation in the lateral and vertical-rotational pile foundation stiffnesses at Bents 61 (in Merritt sand) and 97 (in Bay mud) is established on the basis of the methodology outlined in 1992 by Norris. Assessed lateral behavior is compared with observed response from the California Department of Transportation (Caltrans) lateral pile group load tests at these bents. Differences between stiffnesses corresponding to conditions reflecting the Caltrans tests and those applicable during the Loma Prieta earthquake are discussed. Likewise, differences between the methodology used here and that reflected by FHWA and the Applied Technology Council are pointed out.

Structural dynamic modeling of a highway bridge requires knowledge of the lateral and vertical-rotational stiffnesses of its foundations, which are typically pile foundations. Uncoupled lateral and vertical-rotational pile group stiffnesses are in turn a function, respectively, of the lateral and vertical responses of the individual piles, which can be evaluated via so-called *p-y* and *t-z* analyses. [See the paper by Norris (*1*) for a general overview of such analysis, with reference to case studies, for both nonliquefying and liquefying soil conditions.] It is such lateral and vertical-rotational pile foundation stiffnesses in Merritt sand (at Bent 61) and in Bay mud (at Bent 97) at the Cypress Street viaduct that are sought here.

Unfortunately for the bridge engineer, these stiffnesses are nonlinear—that is, they are displacement or rotation dependent—and a linear dynamic analysis of a bridge will require the choice of boundary element spring stiffnesses that are compatible with the resulting relative displacements or rotations. This means that given the nonlinear variation in the stiffnesses (e.g., at Bents 61 and 97), the bridge engineer must assume a set of stiffness values for a linear model and repeat the dynamic analysis, supplying a new set of stiffness values each time, until the resulting relative displacements yield stiffness values that match the assumed set of values. It is only in this fashion that one would be able to assess the progressive failure of the Cypress Street viaduct, which occurred over just the northern portion of its length.

Although such analysis will require several iterations, unless it is undertaken, correct determination of the distribution of (seismic) load to the structure, the acceleration on the structure, or the forces in the piles (i.e., the shears at the pile tops and from that the maximum moments in the piles) cannot be made. This is clearly demonstrated in a parallel analysis of the nearby Oakland Outer Harbor Wharf (*2*).

G. Norris, R. Siddharthan, and Z. Zafir, Department of Civil Engineering/258, University of Nevada, Reno, Nev. 89557. P. Gowda, 25 Poncetta Drive #118, Daly City, Calif. 94015.

LESSONS LEARNED FROM ASSESSED VERSUS OBSERVED RESPONSE OF OAKLAND OUTER HARBOR WHARF

The California Strong Motion Instrumentation Program (CSMIP) records for the instrumented Oakland Outer Harbor Wharf, located 1.6 km (1 mi) west of the Cypress Street viaduct, provide very important data for the purpose of understanding pile foundation response during an earthquake.

Although the piles at the Oakland Outer Harbor Wharf are different [0.46 m (18 in.) square free-standing precast concrete piles at large spacing] from those at the Cypress Street viaduct, they derive their lateral resistance from a surface layer of Bay mud (as do piles at Bent 97 of the Cypress Street viaduct) and their vertical resistance from point bearing in an underlying dense sand (similar to the piles at Bent 61 in Merritt sand). Therefore, there is something to be gained in the present consideration of foundation response at the Cypress Street viaduct from this more detailed study of the Oakland Outer Harbor Wharf.

In work undertaken by the authors relative to the Oakland Outer Harbor Wharf (*2*), it was found that using free-field motion input and (assessed) compatible lateral and vertical pile stiffnesses, a linear structural dynamic model is capable of providing computed motions on the deck of the wharf that nearly perfectly match the recorded accelerations on the structure. On the other hand, using stiffnesses that are too high (e.g., assuming fixed foundations) causes an assessed peak acceleration (0.58 *g*) twice the recorded acceleration and shear and tensile forces at the head of the critical pile almost three times that of the compatible stiffness solution. Similar combinations of lateral and vertical stiffnesses that are too high or low (as compared with displacement-compatible values) cause poor predicted responses.

An important point in the evaluation of the compatible stiffnesses is that the soil modulus values (Young's *E* or shear modulus *G*) employed in such assessment should be chosen in relation to the governing strain condition in the soil. At present, FHWA (*3*) and Applied Technology Council (ATC) (*4*) recommendations in regard to this matter are at odds. FHWA would have the engineer assess stiffnesses on the basis of traditional *p-y* and *t-z* approaches, where pile responses are a function of the relative displacements, as if the soil immediately surrounding the foundation (the near-field soil),

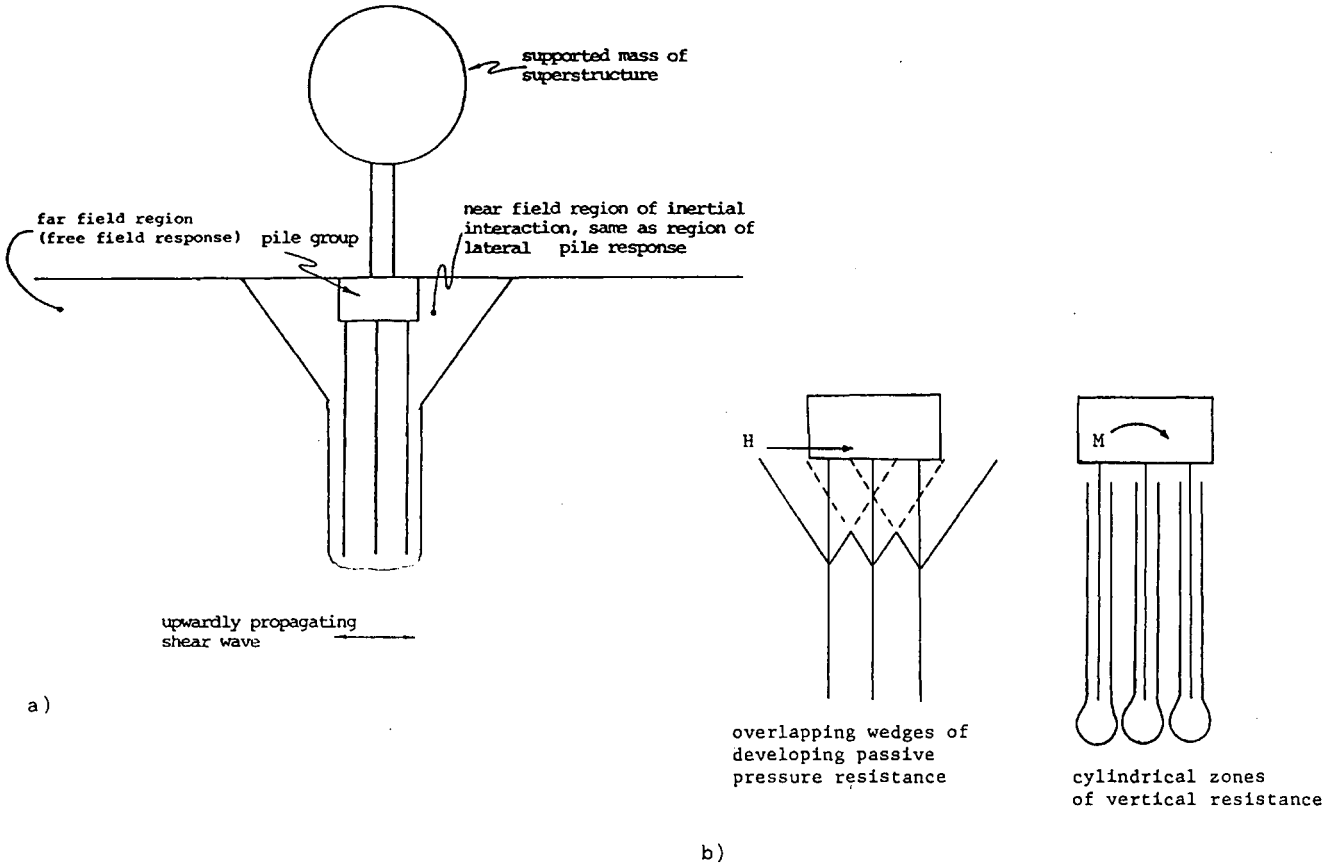

FIGURE 1 (*a*) **Near- versus far- (i.e., free-) field soil regions and** (*b*) **differing near-field (or inertial interaction) soil regions for lateral and vertical pile response.**

as shown in Figure 1a, were moving and the free-field soil (also called the far-field soil) were not. During seismic excitation, this would not be the case. ATC, on the other hand, would have the engineer use soil modulus values based on the level of the free-field strain, as if there were no relative motion in the near-field soil (i.e., the near-field soil moves in an identical manner to the free-field soil).

Of course, the appropriate procedure would be to take the modulus values in the associated near-field soil region, as shown in Figure 1b, as a function of the total strain (free-field plus relative, with due regard to phase differences). However, an expedient that would be more reasonable than either the FHWA or ATC approaches would be to use the larger of the two strains (free-field or relative) in the near-field soil region, that is, assume that either one or the other dominates. However, since the governing relative strain is a function of the level of the inertial interaction response of the superstructure, the engineer does not automatically know which is the larger. Nevertheless, this approach can be accommodated by showing the stiffness, determined as a function of the relative displacement or strain, with a superposed cutoff where the relative displacement or strain would be less than the free-field value.

Figure 2 is such a plot of the nonlinear variation in the vertical pile stiffness at the Oakland Outer Harbor Wharf showing a cutoff at 350 kN/mm (2,000 kips/in.) at a relative vertical pile head movement of 0.75 mm (0.03 in.), corresponding to the equivalent free-field shear strain of 3×10^{-2} percent in the dense sand and 2×10^{-1} percent in the overlying Bay mud. The computer program SHAKE (*5*) was used to obtain these shear strains given the free-field ground surface acceleration record shown in Figure 11 of the preceding paper in this Record. The shear moduli, G, of the soils in the *t-z* program were then limited to the corresponding values from the SHAKE program, resulting in a constant vertical pile head stiffness (350 kN/mm) for relative pile head displacements less than 0.75 mm (i.e., the free-field strain dominates) and a diminishing stiffness at successively greater displacements (i.e., the near-field or inertial interaction strain dominates). By contrast, the FHWA approach would have the stiffness increase at lower displacements (<0.75 mm), whereas the ATC approach would have the stiffness remain constant at 350 kN/mm (i.e., a horizontal line) across all levels of relative displacement. It should be pointed out that in the case of the Oakland Outer Harbor Wharf, the compatible solution resulted in the vertical pile stiffnesses falling (as different points for differently loaded piles) on this horizontal cutoff of 350 kN/mm, whereas the compatible horizontal stiffnesses for all piles fell on their appropriate curve, to the right of the free-field cutoff. In other words, it was the free-field

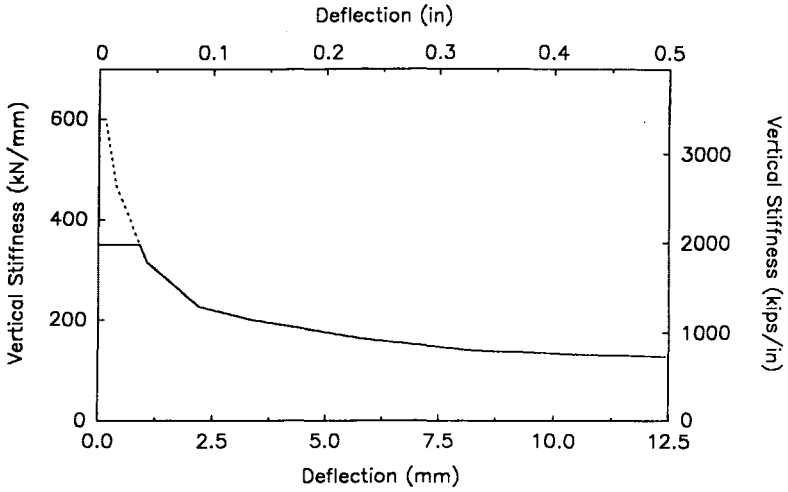

FIGURE 2 Vertical pile stiffness variation for 0.46-m (18-in.) square prestressed concrete piles at Oakland Outer Harbor Wharf during the Loma Prieta earthquake.

strain that governed in the case of the vertical response of the piles and the relative (near-field) strain that governed in the case of the lateral response of the piles.

In the following sections, the vertical-rotational and the lateral response of pile foundations at Bents 61 and 97 of the Cypress Street viaduct are established and compared.

VERTICAL-ROTATIONAL STIFFNESS

Figure 3a and b gives the backbone load-settlement curves assessed for the short end bearing pile in Merritt sand and the long friction pile in the Bay mud at Bents 61 and 97, respectively, on the basis of the soil conditions characterized in Figure 9 (both with and without porewater pressure buildup in the Merritt sand) and Figure 10 of the preceding paper.

The alpha method (*6*), using Tomlinson's average curve for all piles, was used to assess the capacity of the pile [623 kN (140 kips)] in Bay mud. Ramberg-Osgood fitting parameters for the t-z curves and the point load-displacement Q_p-z_p curve were employed relative to the different segments used to assess the undrained capacity of the pile in Bay mud. Given the Ramberg-Osgood fitting parameters for the backbone t-z and Q_p-z_p responses, the unload-reload fitting parameters are automatically known. Such parameters and a very simple t-z analysis program are presented elsewhere (*7*) for the reader's reference relative to such treatment of the pile in the Bay mud.

The Nordlund and Thurman method (*8*) was used to assess the ultimate capacity of the pile in sand [512 kN (115 kips)] based on an estimated drained friction angle of 37 degrees at pile point (and other values varying by pile segment along the pile length). The correlation appearing in NAVFAC DM-7.1 (*9*) was used to establish ϕ from D_r. (The variation in D_r is shown in Figure 9 of the preceding paper.) The t-z analysis used to assess the backbone and unload-reload responses of a pile in the Merritt sand is explained in detail in an associated report (*10*).

The reader should note the difference in the backbone curves of Figure 3b. The curve for the pile under developing porewater pressure conditions (N_{eq} = 4 cycles, corresponding to the end of strong shaking) in clean sand was assessed in the same way as the original curve except that the reduced level of vertical effective stress ($\sigma_{v'} = \sigma_{v'o} - u_{xs}$) was used in place of the original value $\sigma_{v'o}$ (see Figure 9 of the preceding paper). The reduction in effective stress affects the shaft resistance of only a few pile segments. Since point resistance contributes 423 kN (95 kips) of the total 512-kN (115-kip) capacity, such reduction in the shaft resistance [89 kN (20 kips) reduced to 45 kN (10 kips)] does not appear to be significant. However, the fact that the shaft resistance is fully mobilized well before point resistance can build up means that even this small loss in capacity has a noticeable effect in terms of the vertical unload-reload stiffness variation, as discussed below.

Figure 4 shows the unload-reload vertical pile stiffness variations for Bents 97 and 61. The stiffness k_v is simply the ratio of pile head load change ΔQ to the pile head displacement Δz, as discussed by Norris (*1*). The difference in stiffness of piles at Bent 61 with (Figure 4c) and without (Figure 4b) porewater pressure buildup is due to the loss in shaft capacity, which is felt at low levels of deflection because of the early mobilization of the shaft as compared with point resistance. Such difference in response diminishes at higher levels of deflection because of the greater mobilization of the very large point resistance, which was not affected by porewater pressure buildup.

It is important to point out that no cutoffs have been shown on these curves corresponding to the level of free-field strain (see Figure 2) because no free-field response analysis has been undertaken for the Cypress Street viaduct. (Recall from earlier discussion of the Oakland Outer Harbor Wharf that equivalent free-field strains in the dense sand and the overlying layer of Bay mud were almost an order of magnitude different for the same ground surface acceleration.) Therefore, the cutoffs would most likely occur at different values of axial pile displacement for curves in Figure 4a versus those in Figure 4b and c.

Figure 5 shows the transverse stabilized rotational stiffnesses of two similar groups at Bents 61 and 97 established

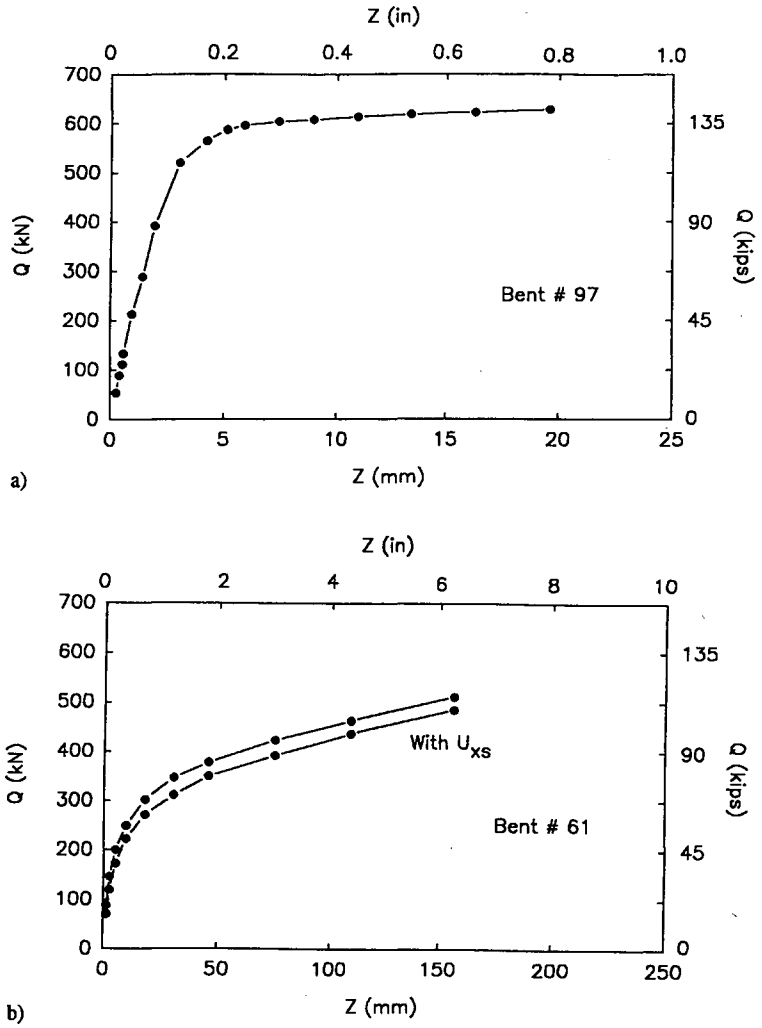

FIGURE 3 Backbone load-settlement curves for piles of (*a*) Bent 97 (long friction piles in Bay mud) and (*b*) Bent 61 (short end bearing piles in Merritt sand).

from the curves of Figure 4 based on the formulation given by Norris (*1*). (Again, note that no free-field cutoff is shown.) These are the center groups of the layout shown in Figure 6 from the paper by Abcarius (*11*). Even though the group at Bent 97 has one more pile, this extra pile falls on the stabilized axis of rotation and would offer little moment resistance. However, it should be pointed out that a shear key was used at the base of the column connection to the foundations, thereby affecting such moment transfer. Therefore, for purposes of comparison, one should really compare the transverse moment resistance of the whole bent in such soils (Bent 61 versus Bent 97), that is, the vertical stiffnesses of the piles of a group multiplied by their vertical pile head displacement multiplied by the distance between pile groups on opposite sides of the bent. (See Figure 1 of the preceding paper.) Of course, in a structural dynamic model, lateral and vertical stiffnesses rather than lateral and rotational stiffnesses would be supplied for each foundation.

Regardless of which it is that one compares—the vertical stiffness of the individual pile, the rotational stiffness of the group, or the rotational stiffness of the bent as a whole—it is clear from Figures 4 and 5 that the long friction piles in Bay mud are stiffer (for the same deflection and rotation) than the short end bearing piles in the Merritt sand.

LATERAL STIFFNESS

The lateral stiffness of a pile group derives from the lateral stiffness of the average pile in the group multiplied by the number of piles, to which one adds the lateral stiffness of the pile cap.

Although no group interference effect is employed relative to the vertical-rotational response of the piles, such an effect needs to be considered relative to laterally loaded pile response. As can be judged from Figure 1b, there is considerable overlap in the developing passive wedges of neighboring piles under lateral load as compared with no overlap of cylindrical zones of soil under vertical-rotational excitation. In addition, although rotational response is assessed for an

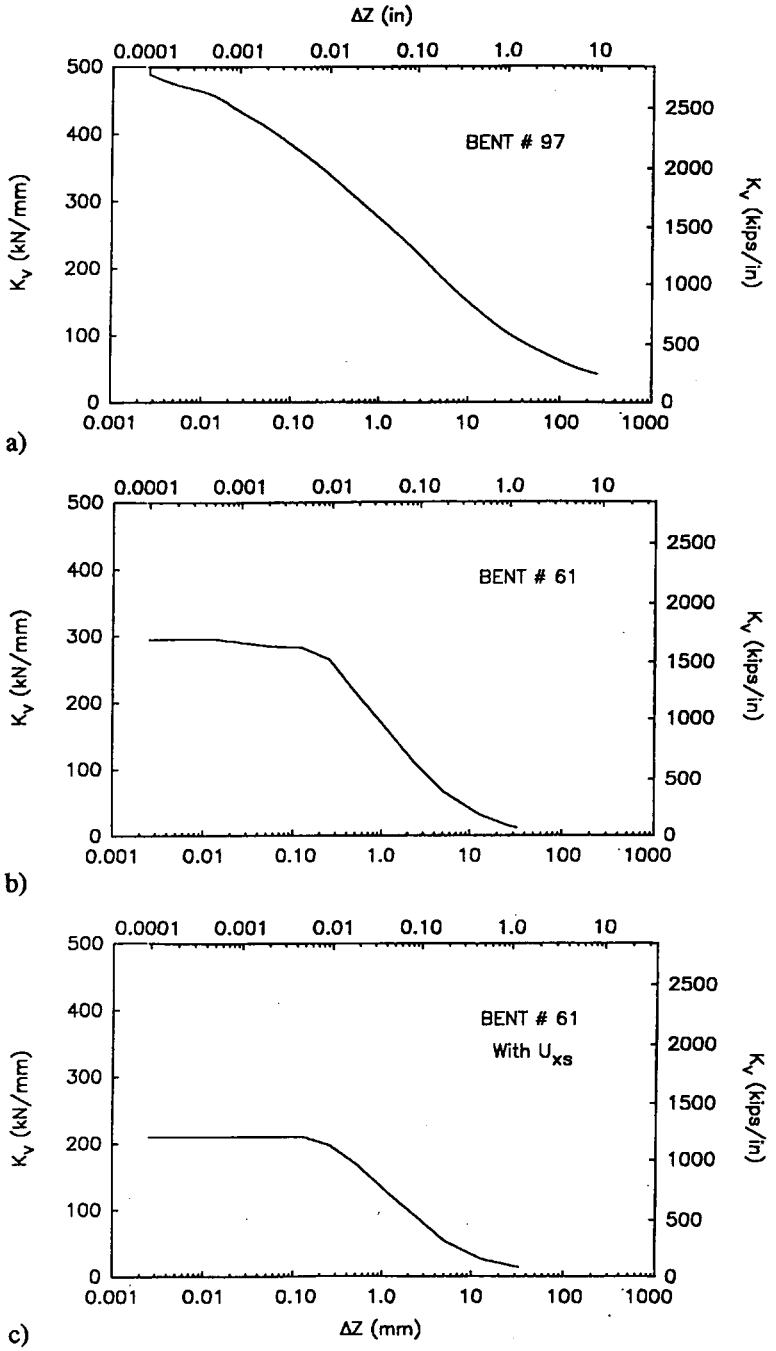

FIGURE 4 Nonlinear variation in the stabilized vertical pile stiffness (*a*) at Bent 97, (*b*) for no porewater pressure buildup (or at the start of strong shaking) at Bent 61, and (*c*) for porewater pressure buildup at the end of strong shaking at Bent 61. (Note that no free-field cutoff is shown.)

implied free (i.e., pinned) head condition, the lateral stiffness will vary depending on the appropriate head fixity condition. Therefore, a number of issues (pile cap contribution, group effect, and head fixity) are part of the lateral stiffness evaluation that are not part of the vertical-rotational stiffness evaluation.

The authors have calculated the lateral response of the individual pile on the basis of the so-called strain wedge model (*12,13*), which relates (*a*) the lateral strain (ε) in the developing passive wedge in front of the pile to the resulting pile deflection pattern (y versus x or deflection δ), (*b*) the horizontal stress change ($\Delta\sigma_h$) to the beam-on-elastic-foundation (BEF) soil-pile reaction (p), and (*c*) the Young's modulus of the soil ($E = \Delta\sigma_h/\varepsilon$) to the BEF subgrade modulus ($E_s = p/y$). Thus, the strain wedge model is a means for relating the one-dimensional BEF model parameters to the (envi-

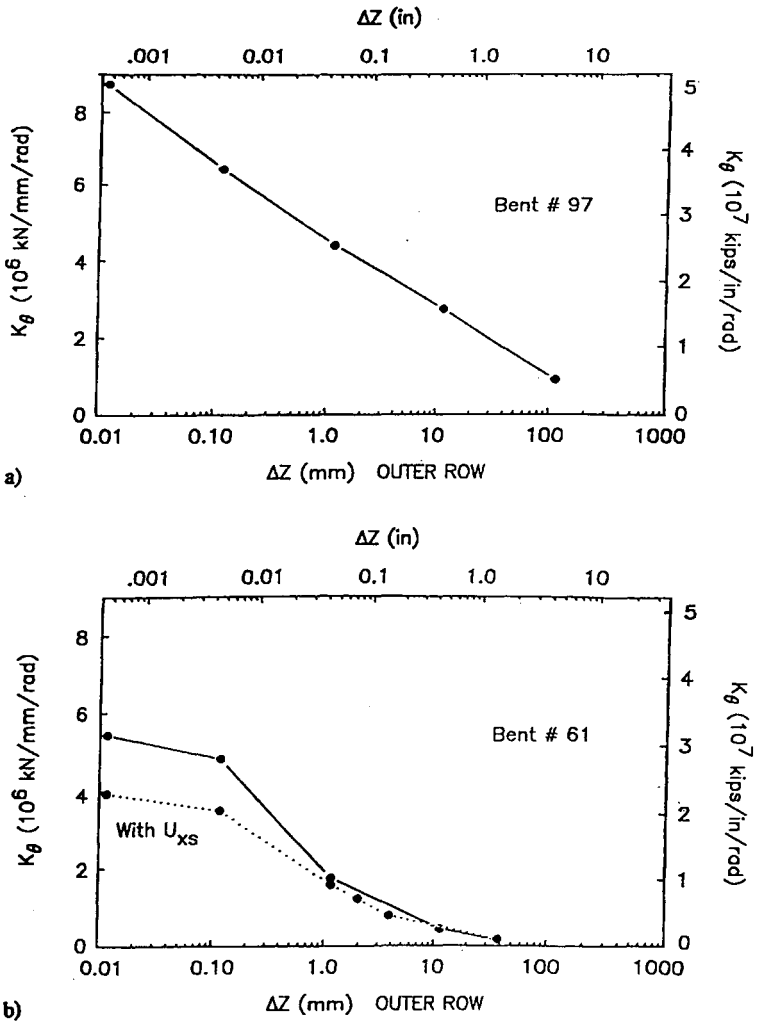

FIGURE 5 Nonlinear variation in the stabilized rotational stiffness of (*a*) 11-pile group at Bent 97 and (*b*) 10-pile group at Bent 61. (No free-field cutoff is shown on either curve.)

sioned) three-dimensional soil-pile response. These relationships ($\delta = \chi\varepsilon$, $E_s = NE$, and $P/B = A\Delta\sigma_h$, where χ, N, and A are the correlation parameters and B is the pile diameter) are shown schematically in Figure 7 at two levels of soil strain (ε) and therefore at two different pile head loads.

An interesting feature of such an approach is that the BEF *p-y* curves can be derived theoretically and have been shown to be in reasonable agreement (for common 1- and 2-ft diameter piles) with the empirical curves that are a part of such programs as COM624 (*14*). However, strain wedge model formulation clearly shows that such *p-y* curves are a function of pile properties as well as soil properties. The pile properties that affect the *p-y* curves are pile size, its bending stiffness *EI*, and the pile head fixity condition. It should be pointed out that the *p-y* curves are merely a by-product of the approach that solves for the Young's modulus profile of the soil for the specified value of horizontal strain. Knowing the pile and soil properties, the BEF subgrade modulus profile is obtained and traditional BEF analysis is invoked. In other words, an equivalent linear subgrade modulus profile results for the horizontal strain assumed.

In three dimensions, it is assumed that the developing passive wedge opens up at a fan angle ϕ_m equal to the mobilized effective stress friction angle of the soil. This is shown in Figure 8. With increasing lateral load, the base of the developing wedge moves down, as does the depth of the first zero crossing of the pile (i.e., the first depth where lateral deflection *y* equals zero). As the wedge moves down, it also opens up as strain and stress change and the mobilized friction angle increases. Given this approach, it is easily understood that a stiff pile (high *EI*) will have a different zero crossing than a flexible pile under the same lateral pile head load and therefore will invoke a different depth of soil to provide the needed (mobilized) lateral passive pressure resistance (or horizontal stress change) required for equilibrium. This horizontal stress change (equivalent to the deviator stress in a triaxial test at a confining pressure equal to the effective overburden pressure, $\sigma_{v'o}$) multiplied by the width of the front of the wedge at that depth is the corresponding BEF line load force *p* at that depth. (In clay, the geometry of the wedge is a function of the mobilized effective stress friction angle, but the stress change and strain are the deviator stress and axial strain from

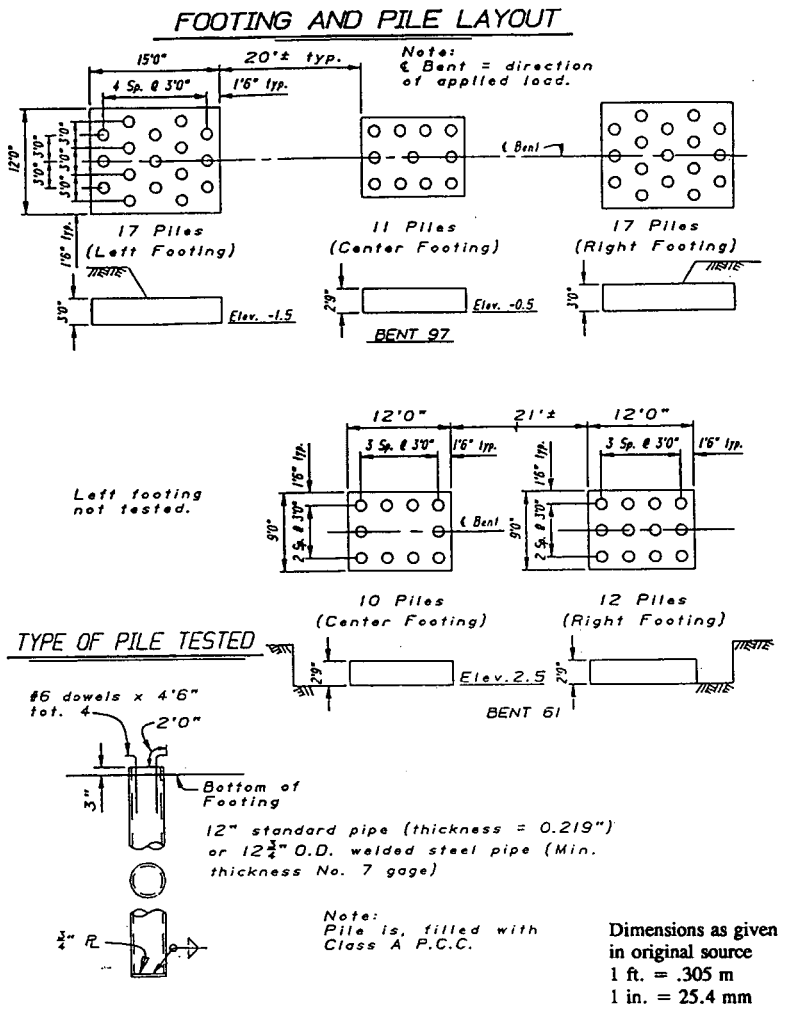

FIGURE 6 Layout of Caltrans pile group load tests [from Abcarius (*11*)]. Groups compared in Figure 5 are the center groups.

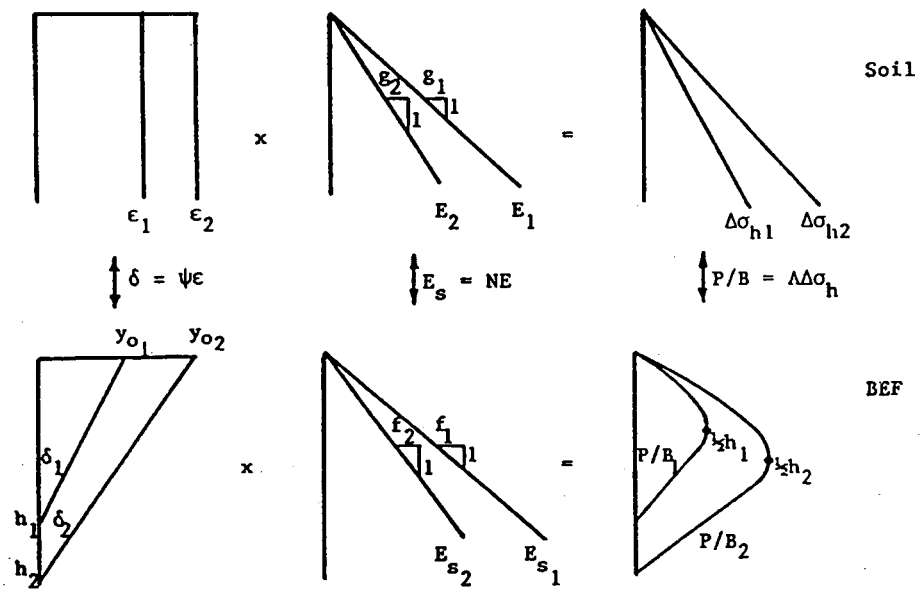

FIGURE 7 Relationship between beam-on-elastic-foundation (BEF) and soil parameters.

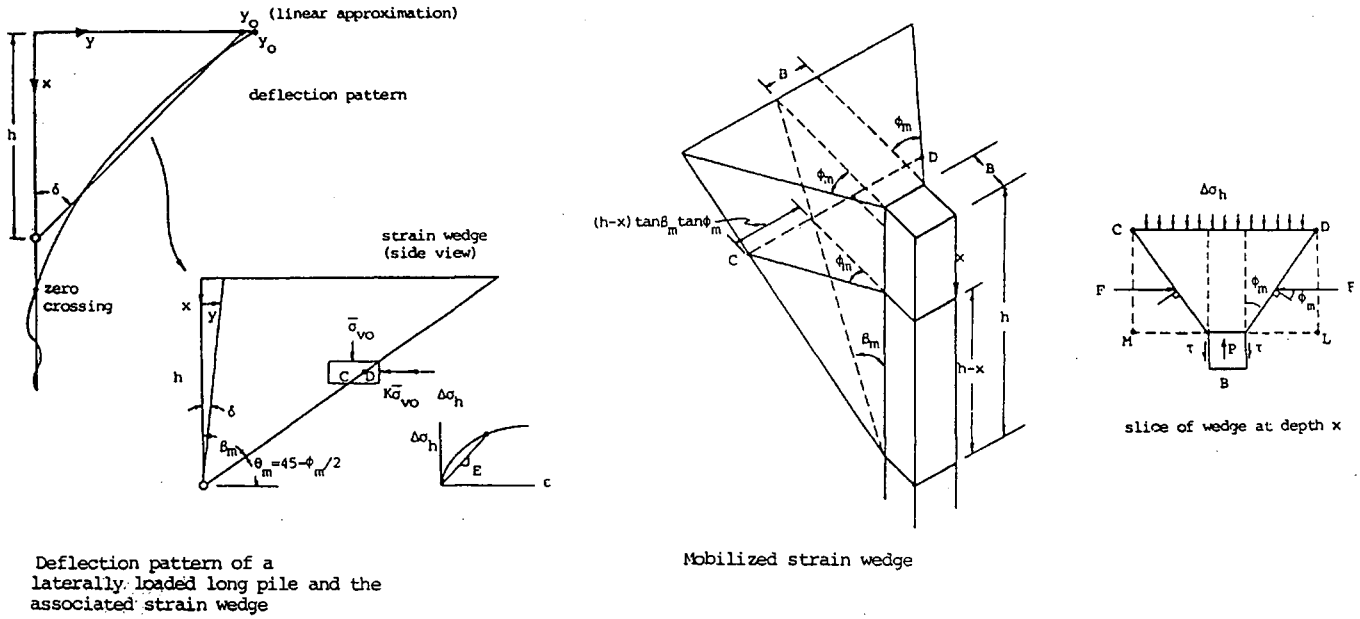

FIGURE 8 Strain wedge model.

a consolidated undrained triaxial test.) Therefore p (as well as deflection y and thereby $E_s = p/y$) at any depth x will be a function of the pile bending stiffness EI (and the pile head fixity condition). Likewise, the p-y curve at a given depth will vary depending upon the soil immediately above and below that in question.

The features that make the strain wedge model particularly useful in the present application are these: (*a*) one knows the value of relative strain in the near-field soil region (i.e., within the wedge) and (*b*) the fact that one determines the equivalent linear subgrade modulus (E_s) profile means that it is a simple matter to reduce it to account for pile group interference effects. [To do the latter, the reduction factor R, given as a function of the center-to-center spacing of the piles, from NAVFAC DM-7.2 (*6*) is employed.] The fact that one knows the value of the (relative) strain allows for a comparison with the level of free-field strain and therefore the establishment of a free-field cutoff. Neither of these features is readily available in programs such as COM624 (*14*). One last feature is that the model is good over the full range in soil strain, from 1×10^{-4} percent up to and beyond soil failure.

Figure 9 shows a comparison of the lateral load response for the same pile groups considered earlier (Figure 6) assessed from lateral pile group load tests conducted by Caltrans at Bents 61 and 97. The details of the tests and the results obtained for the opposing groups (from jacking apart pairs of groups) at these bents are given by Abcarius (*11*). Such tests are unique in that they were carried to structural failure of

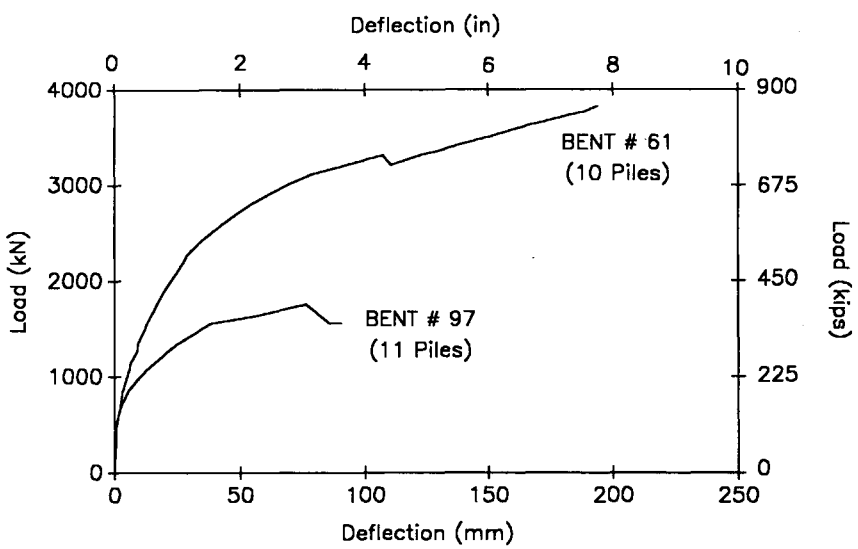

FIGURE 9 Lateral load versus deflection response of 10- and 11-pile groups at Bents 61 and 97 from Caltrans tests.

the piles or cap at very high lateral deflections. It is interesting that the lateral resistance of the pile group in Merritt sand is much greater than that of the pile group in the Bay mud (even with one more pile in the latter group). Recall that the opposite was true relative to the vertical-rotational resistance; that is, the long friction pile group in Bay mud was stiffer in vertical-rotational resistance than the short end bearing group in the Merritt sand. The reason for this reversal is that the soil providing the resistance to the lateral load is different from that offering resistance to the vertical load, as shown schematically in Figure 1b.

Although the load-deflection curves of Figure 9 may be used to construct the variation in lateral stiffness K_{lat} (load divided by deflection) of the group, it is important to see if the same response can be assessed. Accordingly, a strain wedge model program was used to develop the load-versus-deflection response for two pile head fixity conditions, a free (pinned) head condition and a fully fixed condition (deflection with zero rotation at pile top). However, the program STIFF1 (*15*) was used to establish the reduced bending stiffness *EI* that would result from cracking at higher lateral loads, and hence moments, in the pile. From such results, it was determined that the ultimate moment in the pile at pile top would be 470 kN-m (347 kip-ft), whereas at a depth below the upper level of reinforcing steel (see Figure 6) it would be 247 kN-m (182 kip-ft). For the free head pile where the moment is a maximum at the lower level, the bending stiffness *EI* was taken to vary with the value of maximum moment at this lower level M_l. Once a plastic hinge formed (the maximum moment equaled the ultimate moment of 247 kN-m [182 kip-ft] at the lower level), the depth of the developing strain wedge was taken to remain fixed as the soil in the wedge built up to failure. The free head response curves for the two pile groups are shown in Figure 10. Values of *EI* for the corresponding lower-level moments are noted on these curves.

By contrast, the *EI* for the fixed head response was taken to vary with the maximum moment at pile top M_t. However, letting *EI* decrease with the increase in pile head load, and hence maximum moment, eventually led to development of a plastic hinge at pile top. Thereafter, the so-called fixed head condition was solved assuming a constant moment at the pile head [470 kN-m (47 kip-ft)]. Interest then shifted to the maximum moment at the lower level M_l and the eventual development of a second hinge at this location. During this time, the *EI* was taken on the basis of the moment at the lower level. The fixed head curves for such an analysis are also shown in Figure 10.

One can consider each point on the calculated curve or curves at the higher level of load as one point from a line reflecting a load-deflection curve for a pile with a constant

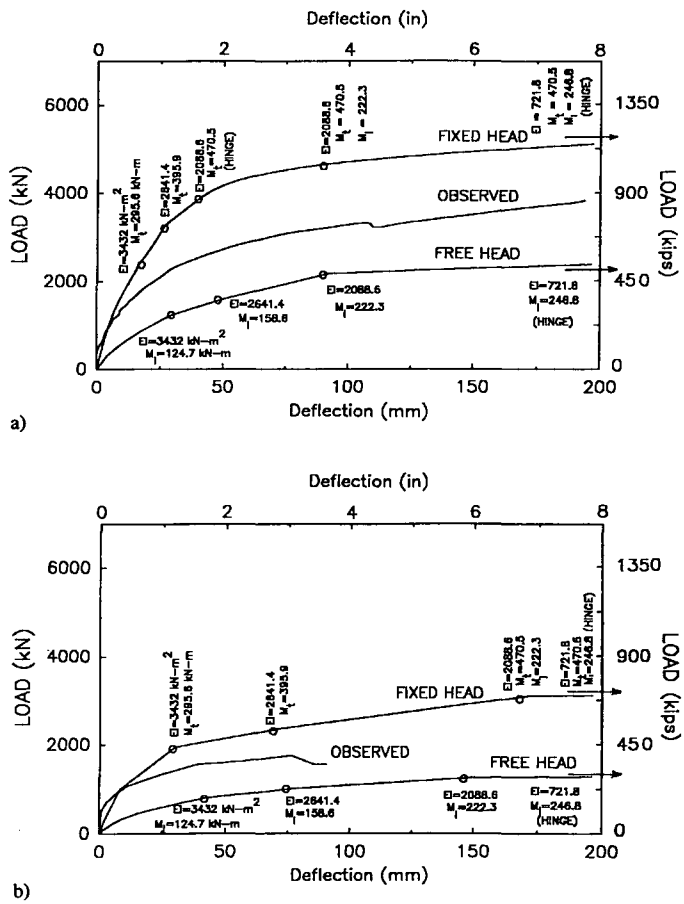

FIGURE 10 Predicted versus observed response of (*a*) 10-member pile group at Bent 61 and (*b*) 11-member pile group at Bent 97.

EI passing through that curve and only that (compatible) point used to establish the final curve. Of course, at lower levels of load a constant *EI* was used.

The observed responses from Figure 9 are plotted in Figure 10 for comparison. It is interesting to note that at low loads the recorded response is stiffer than, but generally follows, the computed fixed head response and then starts to deviate as if the piles were unable to maintain more than a limited pile head moment. The levels of pile head moment at which the observed response deviates from the computed fixed head response are 134 and 138 kN-m (99 and 102 kip-ft) for the pile groups at Bents 61 and 97, respectively. This then represents the yielding of the pile-to-cap connection rather than the failure of the piles. Not shown are the predicted responses in which the pile head moments are limited to these values, curves that virtually overlie their respective observed response.

It should be pointed out that the predicted responses were assessed on the basis of different pile group interference effects. Although the spacing of the piles in the group is not constant (because of missing piles in the arrangement), a weighted value was assessed and an *R*-value chosen accordingly. The *R*-values employed were 0.55 for the 10-pile group of Bent 61 and 0.335 for the 11-pile group of Bent 97.

Although the strain wedge model response was calculated for the large loads to which the tests were carried, it was also used to assess response at very small deflections. At such a level of response, it is clear from Figure 10 that a fixed head condition should be assumed. Likewise, given the growth in both the depth and the breadth of the pile's strain wedge with increasing load (as can be imagined from reference to Figure 8), it is likely that the *R*-value should be higher (for less interference between neighboring wedges) at lower load levels. (However, such additional correction was not attempted here.) Figure 11 shows the variation in the calculated fixed head pile group stiffnesses over the small deflection range. Of course, the free-field cutoff (see Figure 2) has not been superimposed on these plots. However, if one were to employ the free-field strain values for the dense sand and Bay mud at the Oakland Outer Harbor (which are not necessarily the correct values to use at the Cypress Street viaduct because the values at the Oakland Outer Harbor correspond to a common ground surface acceleration), the solid point appearing on each curve would mark the level at which the horizontal line would occur. Note the significant difference in deflections associated with these points.

The reader will note that the soil surrounding the pile caps of the center test groups was removed, and therefore no cap resistance was added in the strain wedge model analysis. By contrast, during the Loma Prieta earthquake, there would have been this additional resistance as well as 0.6 to 0.9 m (2

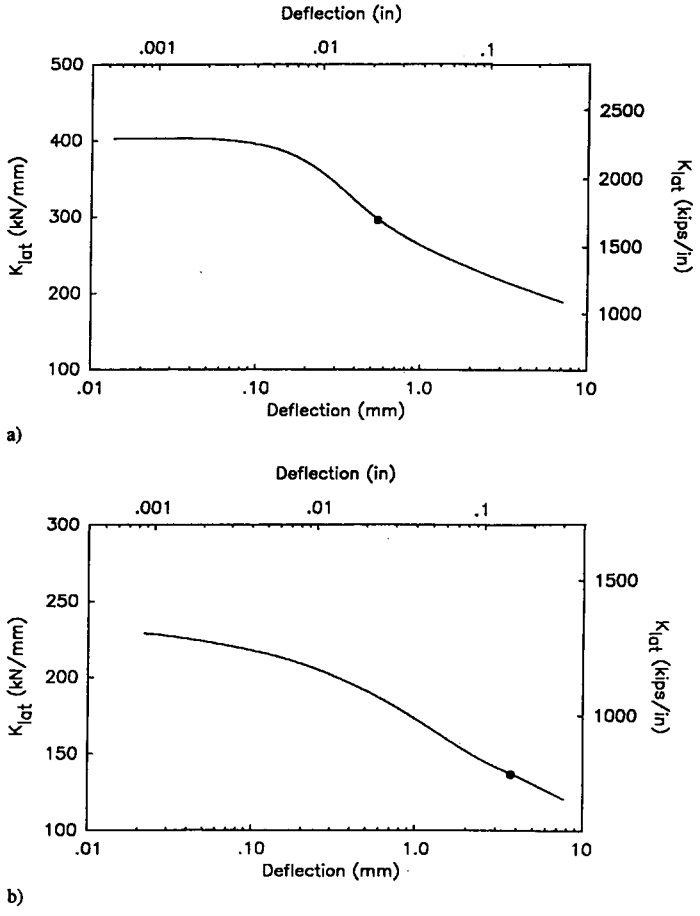

FIGURE 11 Computed lateral stiffness variations in the small deflection range for (*a*) 10-member pile group at Bent 61 and (*b*) 11-member pile group at Bent 97.

to 3 ft) more overburden as compared with that shown in Figures 9 and 10 of the preceding paper.

DISCUSSION OF RESULTS

In this paper, the Cypress Street viaduct failure has been used as a vehicle to highlight present capabilities and shortcomings relative to the evaluation of seismic pile foundation stiffness. A significant point that the authors have tried to make is the need for highway departments to carry through on such "geotechnical" analysis. It is important that in undertaking structural dynamic modeling of a highway bridge, deflection- and rotation-compatible foundation stiffnesses be used in order to assess the motion of the structure appropriately, obtain the correct distribution of seismic loads to the structure, and evaluate foundation (pile head) forces appropriately. It has been shown in parallel soil-foundation-structure analysis relative to the nearby Oakland Outer Harbor Wharf that employing unrealistic stiffnesses can lead to serious errors in the structure's computed motions and the computed foundation forces. This is extremely important with regard to future investments in the seismic retrofit of the nation's bridges.

ACKNOWLEDGMENT

The funding for this study was provided by the U.S. Department of Energy as part of a larger study on pile foundation stiffnesses for the seismic modeling of railroad and highway bridges. Such support is gratefully acknowledged.

REFERENCES

1. Norris, G. M. Overview of Evaluation of Pile Foundation Stiffnesses for Seismic Analysis of Highway Bridges. In *Transportation Research Record 1336*, TRB, National Research Council, Washington, D.C., 1992, pp. 31–42.
2. Norris, G., R. Siddharthan, Z. Zafir, S. Abdel-Ghaffar, and P. Gowda. *Soil-Foundation-Structure Behavior at the Oakland Outer Harbor Wharf.* Report CCEER-91-2. Center for Civil Engineering Earthquake Research, University of Nevada, Reno, 1991.
3. Lam, I. (Po), and G. R. Martin. *Seismic Design of Highway Bridge Foundations.* Reports FHWA/RD-86/101, FHWA/RD-86/102, and FHWA/RD-86/103. FHWA, U.S. Department of Transportation, 1986.
4. *ATC 3-06 Tentative Provisions for the Development of Seismic Regulations for Buildings.* Applied Technology Council, 1978.
5. Schnabel, P. B., J. Lysmer, and H. B. Seed. *SHAKE: A Computer Program for Earthquake Response Analysis of Horizontally Layered Sites.* Report EERC 72-12. Earthquake Engineering Research Center, University of California, Berkeley, 1972.
6. *Design Manual: Foundations and Earth Structures.* NAVFAC DM-7.2. U.S. Government Printing Office, Washington, D.C., 1982, pp. 196 and 241.
7. Norris, G. M. Evaluation of the Nonlinear Stabilized Rotational Stiffness of Pile Groups. In *Proceedings of the 37th Highway Geology Symposium*, Helena, Montana, 1986, pp. 331–386.
8. Vanikar, S. N. *Manual on Design and Construction of Driven Pile Foundations.* Report DP-66-1. FHWA, U.S. Department of Transportation, 1985.
9. *Design Manual: Soil Mechanics.* NAVFAC DM-7.1. U.S. Government Printing Office, Washington, D.C., 1982, p. 149.
10. Norris, G. M., R. Siddharthan, Z. Zafir, and P. Gowda. *Seismic Lateral and Rotational Pile Foundation Stiffnesses at Cypress.* Report CCEER-91-3. Center for Civil Engineering Earthquake Research, University of Nevada, Reno, 1991.
11. Abcarius, J. L. Lateral Load Test on Driven Pile Footings. In *Transportation Research Record 1290*, TRB, National Research Council, Washington, D.C., 1991, Vol. 2, pp. 139–143.
12. Norris, G., and P. Abdollaholiaee. BEF Studies with the Strain Wedge Model. In *Proceedings, 26th Symposium in Engineering Geology and Geotechnical Engineering*, Paper 13, 1990.
13. Norris, G. M., and P. K. Gowda. *Laterally Loaded Pile Analysis for Layered Soil Based on the Strain Wedge Model.* Report 91-3. Center for Civil Engineering Earthquake Research, University of Nevada, Reno, 1991.
14. Reese, L. C., and W. R. Sullivan. *Documentation of the Program COM624.* Geotechnical Engineering Center, Bureau of Engineering Research, University of Texas, Austin, 1980.
15. Wang, S. T., and L. C. Reese. *Documentation of the Program STIFF1: Computation of Nonlinear Stiffnesses and Ultimate Bending Moment of Reinforced-Concrete and Pipe Sections.* Ensoft, Inc., Austin, Texas, 1987.

Publication of this paper sponsored by Committee on Foundations of Bridges and Other Structures.